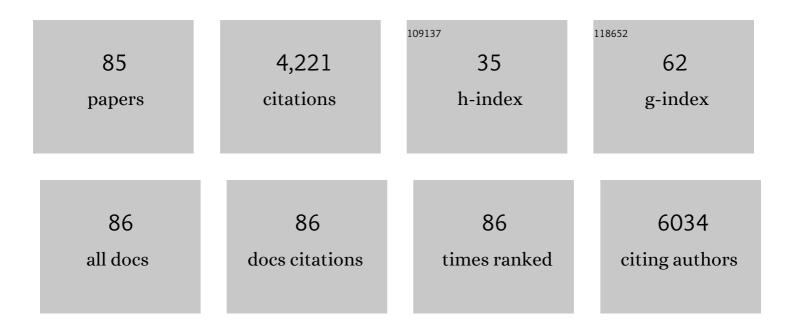
## Xiaojun Zhou

List of Publications by Year in descending order

Source: https://exaly.com/author-pdf/19567/publications.pdf Version: 2024-02-01



#	Article	IF	CITATIONS
1	Flower-like PEGylated MoS2 nanoflakes for near-infrared photothermal cancer therapy. Scientific Reports, 2015, 5, 17422.	1.6	219
2	Effect of pH-Responsive Alginate/Chitosan Multilayers Coating on Delivery Efficiency, Cellular Uptake and Biodistribution of Mesoporous Silica Nanoparticles Based Nanocarriers. ACS Applied Materials & Interfaces, 2014, 6, 8447-8460.	4.0	209
3	BMP-2 Derived Peptide and Dexamethasone Incorporated Mesoporous Silica Nanoparticles for Enhanced Osteogenic Differentiation of Bone Mesenchymal Stem Cells. ACS Applied Materials & Interfaces, 2015, 7, 15777-15789.	4.0	191
4	Three-dimensional porous scaffold by self-assembly of reduced graphene oxide and nano-hydroxyapatite composites for bone tissue engineering. Carbon, 2017, 116, 325-337.	5.4	191
5	Doxorubicin-loaded electrospun poly(l-lactic acid)/mesoporous silica nanoparticles composite nanofibers for potential postsurgical cancer treatment. Journal of Materials Chemistry B, 2013, 1, 4601.	2.9	174
6	Mechanically and biologically skin-like elastomers for bio-integrated electronics. Nature Communications, 2020, 11, 1107.	5.8	162
7	Tannic acid-reinforced methacrylated chitosan/methacrylated silk fibroin hydrogels with multifunctionality for accelerating wound healing. Carbohydrate Polymers, 2020, 247, 116689.	5.1	140
8	Au/Polypyrrole@Fe <sub>3</sub> O <sub>4</sub> Nanocomposites for MR/CT Dual-Modal Imaging Guided-Photothermal Therapy: An <i>in Vitro</i> Study. ACS Applied Materials & Interfaces, 2015, 7, 4354-4367.	4.0	128
9	Polyelectrolyte multilayer functionalized mesoporous silica nanoparticles for pH-responsive drug delivery: layer thickness-dependent release profiles and biocompatibility. Journal of Materials Chemistry B, 2013, 1, 5886.	2.9	122
10	3D-printed IFN-Î <sup>3</sup> -loading calcium silicate-Î <sup>2</sup> -tricalcium phosphate scaffold sequentially activates M1 and M2 polarization of macrophages to promote vascularization of tissue engineering bone. Acta Biomaterialia, 2018, 71, 96-107.	4.1	116
11	Electrophoretic Deposition of Dexamethasone-Loaded Mesoporous Silica Nanoparticles onto Poly( <scp>l</scp> -Lactic Acid)/Poly(Îμ-Caprolactone) Composite Scaffold for Bone Tissue Engineering. ACS Applied Materials & Interfaces, 2016, 8, 4137-4148.	4.0	109
12	One-Pot Synthesis of MoS <sub>2</sub> Nanoflakes with Desirable Degradability for Photothermal Cancer Therapy. ACS Applied Materials & Interfaces, 2017, 9, 17347-17358.	4.0	104
13	Multifunctional Redox-Responsive Mesoporous Silica Nanoparticles for Efficient Targeting Drug Delivery and Magnetic Resonance Imaging. ACS Applied Materials & Interfaces, 2016, 8, 33829-33841.	4.0	102
14	In vitro and in vivo toxicity studies of copper sulfide nanoplates for potential photothermal applications. Nanomedicine: Nanotechnology, Biology, and Medicine, 2015, 11, 901-912.	1.7	93
15	Three-dimensional bioprinting of multicell-laden scaffolds containing bone morphogenic protein-4 for promoting M2 macrophage polarization and accelerating bone defect repair in diabetes mellitus. Bioactive Materials, 2021, 6, 757-769.	8.6	91
16	Dual-Responsive Mesoporous Silica Nanoparticles Mediated Codelivery of Doxorubicin and Bcl-2 SiRNA for Targeted Treatment of Breast Cancer. Journal of Physical Chemistry C, 2016, 120, 22375-22387.	1.5	88
17	Mesoporous silica nanoparticles for tissueâ€engineering applications. Wiley Interdisciplinary Reviews: Nanomedicine and Nanobiotechnology, 2019, 11, e1573.	3.3	87
18	Controllable fabrication of hydroxybutyl chitosan/oxidized chondroitin sulfate hydrogels by 3D bioprinting technique for cartilage tissue engineering. Biomedical Materials (Bristol), 2019, 14, 025006.	1.7	84

#	Article	IF	CITATIONS
19	Cartilage-targeting peptide-modified dual-drug delivery nanoplatform with NIR laser response for osteoarthritis therapy. Bioactive Materials, 2021, 6, 2372-2389.	8.6	82
20	Marriage of Albumin–Gadolinium Complexes and MoS <sub>2</sub> Nanoflakes as Cancer Theranostics for Dual-Modality Magnetic Resonance/Photoacoustic Imaging and Photothermal Therapy. ACS Applied Materials & Interfaces, 2017, 9, 17786-17798.	4.0	81
21	<i>In vitro</i> and <i>in vivo</i> studies of a gelatin/carboxymethyl chitosan/LAPONITE® composite scaffold for bone tissue engineering. RSC Advances, 2017, 7, 54100-54110.	1.7	75
22	Bi-layered electrospun nanofibrous membrane with osteogenic and antibacterial properties for guided bone regeneration. Colloids and Surfaces B: Biointerfaces, 2019, 176, 219-229.	2.5	75
23	Bone Microenvironmentâ€Mimetic Scaffolds with Hierarchical Microstructure for Enhanced Vascularization and Bone Regeneration. Advanced Functional Materials, 2022, 32, .	7.8	70
24	Mesoporous silica nanoparticles/gelatin porous composite scaffolds with localized and sustained release of vancomycin for treatment of infected bone defects. Journal of Materials Chemistry B, 2018, 6, 740-752.	2.9	62
25	Merging metal organic framework with hollow organosilica nanoparticles as a versatile nanoplatform for cancer theranostics. Acta Biomaterialia, 2019, 86, 406-415.	4.1	59
26	Facile synthesis of novel albumin-functionalized flower-like MoS <sub>2</sub> nanoparticles for in vitro chemo-photothermal synergistic therapy. RSC Advances, 2016, 6, 13040-13049.	1.7	56
27	Heparinized <scp>PLLA/PLCL</scp> nanofibrous scaffold for potential engineering of smallâ€diameter blood vessel: Tunable elasticity and anticoagulation property. Journal of Biomedical Materials Research - Part A, 2015, 103, 1784-1797.	2.1	54
28	Synthesis and characterization of poly(glycerol sebacate)-based elastomeric copolyesters for tissue engineering applications. Polymer Chemistry, 2016, 7, 2553-2564.	1.9	50
29	Fabrication of heterogeneous porous bilayered nanofibrous vascular grafts by two-step phase separation technique. Acta Biomaterialia, 2018, 79, 168-181.	4.1	50
30	Mussel-Inspired Nanostructures Potentiate the Immunomodulatory Properties and Angiogenesis of Mesenchymal Stem Cells. ACS Applied Materials & Interfaces, 2019, 11, 17134-17146.	4.0	50
31	Construction of nanofibrous scaffolds with interconnected perfusable microchannel networks for engineering of vascularized bone tissue. Bioactive Materials, 2021, 6, 3254-3268.	8.6	48
32	Construction of 3D printed constructs based on microfluidic microgel for bone regeneration. Composites Part B: Engineering, 2021, 223, 109100.	5.9	43
33	3D bioprinted gelatin/gellan gum-based scaffold with double-crosslinking network for vascularized bone regeneration. Carbohydrate Polymers, 2022, 290, 119469.	5.1	43
34	Strontium-incorporated mineralized PLLA nanofibrous membranes for promoting bone defect repair. Colloids and Surfaces B: Biointerfaces, 2019, 179, 363-373.	2.5	39
35	Synthesis of hollow mesoporous silica nanoparticles with tunable shell thickness and pore size using amphiphilic block copolymers as core templates. Dalton Transactions, 2014, 43, 11834.	1.6	38
36	Tumor cell membrane-camouflaged responsive nanoparticles enable MRI-guided immuno-chemodynamic therapy of orthotopic osteosarcoma. Bioactive Materials, 2022, 17, 221-233.	8.6	38

#	Article	IF	CITATIONS
37	Reactive Oxygen Species-Based Biomaterials for Regenerative Medicine and Tissue Engineering Applications. Frontiers in Bioengineering and Biotechnology, 2021, 9, 821288.	2.0	37
38	Porous nanofibrous scaffold incorporated with S1P loaded mesoporous silica nanoparticles and BMP-2 encapsulated PLGA microspheres for enhancing angiogenesis and osteogenesis. Journal of Materials Chemistry B, 2018, 6, 6731-6743.	2.9	35
39	Incorporation of dexamethasone-loaded mesoporous silica nanoparticles into mineralized porous biocomposite scaffolds for improving osteogenic activity. International Journal of Biological Macromolecules, 2020, 149, 116-126.	3.6	35
40	3D bioprinting of proangiogenic constructs with induced immunomodulatory microenvironments through a dual cross-linking procedure using laponite incorporated bioink. Composites Part B: Engineering, 2022, 229, 109399.	5.9	33
41	Interleukin-35 Inhibits TNF-α-Induced Osteoclastogenesis and Promotes Apoptosis via Shifting the Activation From TNF Receptor-Associated Death Domain (TRADD)–TRAF2 to TRADD–Fas-Associated Death Domain by JAK1/STAT1. Frontiers in Immunology, 2018, 9, 1417.	2.2	32
42	Construction of a nanofiber network within 3D printed scaffolds for vascularized bone regeneration. Biomaterials Science, 2021, 9, 2631-2646.	2.6	32
43	Localized delivery of FTY-720 from 3D printed cell-laden gelatin/silk fibroin composite scaffolds for enhanced vascularized bone regeneration. Smart Materials in Medicine, 2022, 3, 217-229.	3.7	32
44	Electrospun nanofibers incorporating self-decomposable silica nanoparticles as carriers for controlled delivery of anticancer drug. RSC Advances, 2015, 5, 65897-65904.	1.7	31
45	Controlled release of vancomycin from 3D porous graphene-based composites for dual-purpose treatment of infected bone defects. RSC Advances, 2017, 7, 2753-2765.	1.7	31
46	Strontium-doped gelatin scaffolds promote M2 macrophage switch and angiogenesis through modulating the polarization of neutrophils. Biomaterials Science, 2021, 9, 2931-2946.	2.6	31
47	Biodegradable Mesoporous Silica Nanocarrier Bearing Angiogenic QK Peptide and Dexamethasone for Accelerating Angiogenesis in Bone Regeneration. ACS Biomaterials Science and Engineering, 2019, 5, 6766-6778.	2.6	28
48	Macroporous nanofibrous vascular scaffold with improved biodegradability and smooth muscle cells infiltration prepared by dual phase separation technique. International Journal of Nanomedicine, 2018, Volume 13, 7003-7018.	3.3	27
49	Interactions between activated sludge extracellular polymeric substances and model carrier surfaces in WWTPs: A combination of QCM-D, AFM and XDLVO prediction. Chemosphere, 2020, 253, 126720.	4.2	26
50	Versatile Nanocarrier Based on Functionalized Mesoporous Silica Nanoparticles to Codeliver Osteogenic Gene and Drug for Enhanced Osteodifferentiation. ACS Biomaterials Science and Engineering, 2019, 5, 710-723.	2.6	25
51	Radiation Induces Apoptosis and Osteogenic Impairment through miR-22-Mediated Intracellular Oxidative Stress in Bone Marrow Mesenchymal Stem Cells. Stem Cells International, 2018, 2018, 1-16.	1.2	22
52	Bilayered Scaffold Prepared from a Kartogenin-Loaded Hydrogel and BMP-2-Derived Peptide-Loaded Porous Nanofibrous Scaffold for Osteochondral Defect Repair. ACS Biomaterials Science and Engineering, 2019, 5, 4564-4573.	2.6	22
53	Tumor-targeted biodegradable multifunctional nanoparticles for cancer theranostics. Chemical Engineering Journal, 2019, 378, 122171.	6.6	22
54	Manganese-doped gold core mesoporous silica particles as a nanoplatform for dual-modality imaging and chemo-chemodynamic combination osteosarcoma therapy. Nanoscale, 2021, 13, 5077-5093.	2.8	22

#	Article	IF	CITATIONS
55	A new model for the electrical conductivity of cement-based material by considering pore size distribution. Magazine of Concrete Research, 2017, 69, 1067-1078.	0.9	19
56	Carbohydrate metabolism and gene regulation during anther development in an androdioecious tree, Tapiscia sinensis. Annals of Botany, 2017, 120, 967-977.	1.4	19
57	3D bioprinting of osteon-mimetic scaffolds with hierarchical microchannels for vascularized bone tissue regeneration. Biofabrication, 2022, 14, 035008.	3.7	18
58	Barrier heights of hydrogen-transfer reactions with diffusion quantum monte carlo method. Journal of Computational Chemistry, 2017, 38, 798-806.	1.5	16
59	Nanosonosensitizers With Ultrasound-Induced Reactive Oxygen Species Generation for Cancer Sonodynamic Immunotherapy. Frontiers in Bioengineering and Biotechnology, 2021, 9, 761218.	2.0	16
60	Local Delivery of BMP-2 from Poly(lactic-co-glycolic acid) Microspheres Incorporated into Porous Nanofibrous Scaffold for Bone Tissue Regeneration. Journal of Biomedical Nanotechnology, 2017, 13, 1446-1456.	0.5	14
61	Aggregation and deposition behaviors of dissolved black carbon with coexisting heavy metals in aquatic solution. Environmental Science: Nano, 2020, 7, 2773-2784.	2.2	13
62	Impacts of carrier properties, environmental conditions and extracellular polymeric substances on biofilm formation of sieved fine particles from activated sludge. Science of the Total Environment, 2020, 731, 139196.	3.9	13
63	Vascularized nanocomposite hydrogel mechanically reinforced by polyelectrolyte-modified nanoparticles. Journal of Materials Chemistry B, 2022, 10, 5439-5453.	2.9	13
64	Performance of the Diffusion Quantum Monte Carlo Method with a Single-Slater-Jastrow Trial Wavefunction Using Natural Orbitals and Density Functional Theory Orbitals on Atomization Energies of the Gaussian-2 Set. Journal of Physical Chemistry A, 2019, 123, 3809-3817.	1.1	12
65	Patient-specific Scaffolds with a Biomimetic Gradient Environment for Articular Cartilage–Subchondral Bone Regeneration. ACS Applied Bio Materials, 2020, 3, 4820-4831.	2.3	12
66	Coupling metal organic frameworks with molybdenum disulfide nanoflakes for targeted cancer theranostics. Biomaterials Science, 2021, 9, 3306-3318.	2.6	12
67	Synthesis and characterization of nanofibrous hollow microspheres with tunable size and morphology via thermally induced phase separation technique. RSC Advances, 2015, 5, 61580-61585.	1.7	11
68	One-step synthesis of multifunctional nanoparticles for CT/PA imaging guided breast cancer photothermal therapy. Colloids and Surfaces B: Biointerfaces, 2021, 201, 111630.	2.5	11
69	Polymeric Nanosystems for Immunogenic Cell Deathâ€Based Cancer Immunotherapy. Macromolecular Bioscience, 2021, 21, e2100075.	2.1	10
70	Fixed-Node Diffusion Quantum Monte Carlo Method on Dissociation Energies and Their Trends for R–X Bonds (R = Me, Et, <i>i</i> -Pr, <i>t</i> -Bu). Journal of Physical Chemistry A, 2018, 122, 5050-5057.	1.1	9
71	Inhibition of Sympathetic Activation by Delivering Calcium Channel Blockers from a 3D Printed Scaffold to Promote Bone Defect Repair. Advanced Healthcare Materials, 2022, 11, .	3.9	8
72	Thermo-and pH dual-responsive mesoporous silica nanoparticles for controlled drug release. Journal of Controlled Release, 2015, 213, e69-e70.	4.8	7

#	Article	IF	CITATIONS
73	Analytical energy gradients for ionized states using equation-of-motion coupled-cluster theory with spin-orbit coupling. Journal of Chemical Physics, 2019, 150, 154114.	1.2	6
74	The opposite functions of miRâ€24 in the osteogenesis and adipogenesis of adiposeâ€derived mesenchymal stem cells are mediated by the HOXB7/βâ€catenin complex. FASEB Journal, 2020, 34, 9034-9050.	0.2	6
75	Design of a Subway Station Crossing Urban Trunk Road by Open Cut and Tunneling Method. , 2013, , .		5
76	Singlet–triplet gaps in diradicals obtained with diffusion quantum Monte Carlo using a Slater–Jastrow trial wavefunction with a minimum number of determinants. Physical Chemistry Chemical Physics, 2019, 21, 20422-20431.	1.3	4
77	Research Update on Bioreactors Used in Tissue Engineering. Journal of Shanghai Jiaotong University (Science), 2021, 26, 272-283.	0.5	4
78	Evaluation of Interleukin-4-Loaded Sodium Alginate–Chitosan Microspheres for Their Support of Microvascularization in Engineered Tissues. ACS Biomaterials Science and Engineering, 2021, 7, 4946-4958.	2.6	4
79	Hypochlorous acid triggered fluorescent probes for <i>in situ</i> imaging of a psoriasis model. Journal of Materials Chemistry B, 2022, 10, 5211-5217.	2.9	4
80	Study on Structural Design and Construction Procedure for a Triple Arch Railway Tunnel. , 2013, , .		3
81	A drug delivery system based on novel hollow mesoporous silica nanospheres. Journal of Controlled Release, 2015, 213, e108-e109.	4.8	3
82	Research Center of 3D Bioprinting in Shanghai Ninth People's Hospital. Bio-Design and Manufacturing, 2019, 2, 213-220.	3.9	1
83	A novel bit-error indicating scheme using only one judge threshold. Science Bulletin, 2009, 54, 3674-3678.	1.7	0
84	Spectral Compression of Femtosecond Soliton in a Dispersion-Increasing Fiber. , 2009, , .		0
85	Cover Image, Volume 11, Issue 6. Wiley Interdisciplinary Reviews: Nanomedicine and Nanobiotechnology, 2019, 11, e1597.	3.3	Ο